Many-body electron origin for the forced magnetostriction in iron-rich Y_2Fe_{17} and $Y_2Fe_{14}B$ itinerant ferromagnets

A. del Moral, C. Abadía, and B. García-Landa
Departmento de Magnetismo de Sólidos, Departamento de Física de Materia Condensada and Instituto de Ciencia de Materiales de Aragón, Universidad de Zaragoza and Consejo Superior de Investigaciones Científicas, 50009 Zaragoza, Spain
(Received 22 October 1999)

We report on the observed high-field (up to 30 T) volume, $\partial \in^{\alpha,1}/\partial H$, and shape, $\partial \in^{\alpha,2}/\partial H$, forced magnetostrictions in the iron-rich Y_2Fe_{17} and $Y_2Fe_{14}B$ itinerant uniaxial intermetallics. The magnetostrictions, which increase rapidly with temperature, are rather strong if compared with iron metal, amounting (in $10^{-6}\,T^{-1}$) for $Y_2Fe_{14}B$ up to $\cong 37$ and $\cong -2.2$ and for Y_2Fe_{17} up to 82 and 15, respectively. A simple Hubbard-like model of forced magnetostriction, within the Hartree-Fock approximation, has been developed in order to interpret the experiments. The most significant result is that the dominant mechanism for forced magnetostriction in those ferromagnets is the strong strain dependence of the $3d$ intraband *effective many-body* electron Coulomb repulsion potential, U^{eff}, which amounts to (in eV Fe atom) $\partial U^{\text{eff}}/\partial \in^{\alpha,1} \cong -(0.12 \pm 0.01)$ and $\partial U^{\text{eff}}/\partial \in^{\alpha,2} \cong 0.04 \pm 0.01$ for $Y_2Fe_{14}B$, and $-(0.04 \pm 0.002)$ and $-(0.006 \pm 3 \times 10^{-4})$ for Y_2Fe_{17}, respectively. The origin for this effective potential strain dependence is mainly related to the strain dependence of the $3d$ electron bandwidth. Dependencies of magnetization and high-field susceptibility with strictions also play a substantial role.

I. INTRODUCTION

The understanding of the mechanisms responsible for the paraprocess or forced *magnetization* (FM) in Fe, Co, and Ni metals and their alloys is one of the classical problems in magnetism.[1–3] The difficulty is double. On one side is the difficulty in measuring accurately enough such a tiny effect in the ''classical'' metals Fe, Co, Ni, and their alloys.[1,4,5] For instance, in iron metal the high-field susceptibility at 286.5 K and 20 T amounts only to (in μ_B/T Fe atom) $\chi_{\text{hf}} = 0.775 \times 10^{-3}$, decreasing down to 0.340×10^{-3}, at 4.2 K.[4] On the theoretical side the situation is rather unclear, and it has been conjectured to be a property mainly related to many-body electron interaction in the ferromagnets.[2,3,6] This theoretical problem has not been fully solved yet and it is not our aim in this work to deal with it in a direct way. Rather, our approach is to investigate another effect very closely related to the FM process: the *forced magnetostriction* (FMS), i.e., the magnetostriction which develops beyond the domain-wall motion and eventually coherent rotation of magnetization out of the easy magnetization direction.[1] In pure $3d$ metals this effect is relatively weak and again somehow difficult to measure with good accuracy.[1,7] For instance, in iron metal at 300 K it amounts to $\partial\omega/\partial H \cong 0.5\text{–}1.5 \times 10^{-6}\,T^{-1}$ and $\partial\lambda[100]/\partial H \cong 0.5\text{–}1 \times 10^{-6}\,T^{-1}$, for the volume and shape (along the easy [100] axis) strictions, respectively.[7] However, we have found that the volume FMS is rather *strong*, between one and two orders of magnitude larger, for the present uniaxial intermetallics Y_2Fe_{17} and $Y_2Fe_{14}B$ and therefore amenable to be measured with much better accuracy. These compounds crystallize in the $P6_3/mmc$ and $P4_2/mnm$ space groups for Y_2Fe_{17} and $Y_2Fe_{14}B$, respectively, and order ferromagnetically below $T_c \cong 310$ and 571 K, respectively.[8,9] Besides, we have found that a sizeable shape striction (c/a ratio distortion) is also developed as mentioned before. To deal with our experimental findings a simple model has been developed, in order to gain some more insight into the FMS origin. Even so, our model does not pursue an *ab initio* calculation of FMS but just attempts to find a relation between the easy direction high-field susceptibility χ_{hf} and magnetization m, and the field dependence of FMS, amenable to comparing with the experimental results. This, in principle, should allow one to extract useful information about the interaction(s) responsible for the FMS.

Several workers have discussed the physical origins of the FM and FMS effects. Holstein and Primakoff[10] first and Pauthenet,[4] more recently, ascribed most of FM in iron metal to spin-wave suppression by the applied magnetic field, although a further contribution, linear in the applied magnetic field H_a, was clearly identified.[4] The spin-wave calculation of del Moral and Brooks[11] predicted that the forced striction should evolve with the applied magnetic field H_a as $\lambda = a_{\text{SW}}\sqrt{H_a}$, for moderate H_a although larger than the anisotropy field H_K, our present situation (a_{SW} is a parameter proportional to T, the temperature). However, such a calculation was in principle only intended for *localized* magnetic moments. Indeed, spin-wave excitations have been observed in Y_2Fe_{17} (Ref. 12) and in $Y_2Fe_{14}B$ (Ref. 13), although at our largest applied magnetic fields (up to 30 T), such a contribution to FMS should be of minor importance in those intermetallics. In fact, it is well known that beyond a certain electron wave-vector limit, which decreases with increasing $H_K + H_a$ field, spin waves are strongly damped because single-particle Stoner excitations take over.[14] We will discuss more about this point later on. We will also show that the observed high-field linear dependence of FMS with H_a has a rather different origin.

The phenomenological model of forced magnetostriction in itinerant ferromagnets that was set forward by Wohlfarth[15] shows that if the magnetic free energy, referred to the para-

magnetic regime, is assumed to be $\Delta F_m(\omega) = -M\,\omega m(T)^2$, where M is the relevant magnetoelastic (MEL) coupling parameter, $m(T)$ the magnetization, and ω the volume strain, from minimization of $\Delta F_m(\omega) + (\frac{1}{2})C\omega^2$, where C is the bulk modulus, it is immediately deduced that the FMS susceptibility becomes

$$\frac{\partial \omega}{\partial H} = \left(\frac{2M}{C}\right)\chi_{\mathrm{hf}}(T)m(T). \tag{1.1}$$

This relationship was later obtained, within the limitations of the Stoner-Wohlfarth rigid band model, by Katsuki and Terao,[16] although the specific and basic interaction underlying the FMS was not fully transparent by that time and Eq. (1.1) was obtained under less basic underground assumptions than our model ones, as we will see below.

The organization of the paper is as follows. In Sec. II we present the experimental results, in Sec. III we develop a model of FMS for itinerant ferromagnets, in Sec. IV we compare the model with experiment, and in Sec. V we discuss some results and extract the main conclusions.

II. EXPERIMENTAL TECHNIQUES AND RESULTS

The magnetostriction measurements were performed in strong pulsed magnetic fields of up to 31 T, available at the High Magnetic Field Facility of Zaragoza University-CSIC,[17] in the range 4–300 K, on single crystals of the above-mentioned intermetallics. The pulse width was $\cong$2.5 sec with rising time of 0.16 sec, the measurements being performed at the decaying period of the pulse, to avoid eddy current and magnetic relaxation effects. The strictions were measured by the well-known strain gauge (SG) technique,[18] using an ac bridge which compensated for the SG magnetoresistance (MR). The SG MR is rather substantial at so intense magnetic fields and low temperatures[19] and extreme care was exercised in order to compensate it. The overall technique had a strain sensitivity of about $\pm 5 \times 10^{-6}$. The magnetic field $\mathbf{H_a}$ was applied along the crystal *easy* magnetization directions, **a** axis for hexagonal Y_2Fe_{17} (2-17 hereafter) and basal-plane **c** axis for tetragonal $Y_2Fe_{14}B$ (2-14 hereafter), as we wanted to obtain the FMS as pure as possible. In both cases, the strains were measured along **a**, **b**, and **c** axes. In this way we were able to determine the α-representation irreducible strictions (IS) for uniaxial symmetry: $\in^{\alpha,1}(\mathbf{ea}) = \in_{xx} + \in_{yy} + \in_{zz}$, i.e., the volume striction; $\in^{\alpha,2}(\mathbf{ea}) = (\sqrt{3}/2)\,(\in_{zz} - (1/3) \in^{\alpha,1}(\mathbf{ea}))$, i.e., the tetragonal or shape striction, which distorts the c/a ratio.[20,21] The Cartesian strains $\in_{ij}$ are referred to the crystal axes with $\hat{\mathbf{x}} \| \mathbf{a}$, $\hat{\mathbf{y}} \| \mathbf{b}$ and $\hat{\mathbf{z}} \| \mathbf{c}$ for the hexagonal lattice cell; for the tetragonal cell $\mathbf{a} \equiv \mathbf{b}$. **ea** means the easy magnetization axis, for applying $\mathbf{H_a}$.

Magnetization measurements, along the **c** and **a** easy axes for 2-14 and 2-17 compounds, respectively, were performed using the well-known induction technique, using concentric well balanced pickup coils. The accuracy of our method is $\cong \pm 1\%$ and the sensitivity $\cong 10^{-3}$ emu ($\cong 10^{-4}\mu_B$).

The sample single crystals were grown by the well-known Czokralsky technique. They were x-ray back-Laue oriented and cut in the form of prisms by spark erosion, with their surfaces containing the lattice cell main crystallographic axes. They were big enough to cement on them our miniature SG (Micromeasurements-350) for magnetostriction measurements.

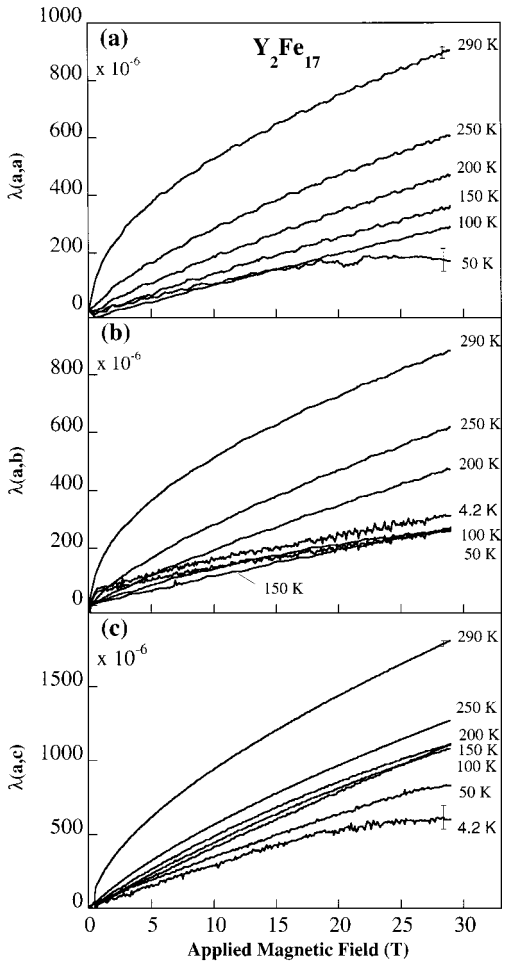

FIG. 1. Magnetostriction isotherms of Y_2Fe_{17} intermetallic compound for the magnetic field applied along the **a** easy direction, measured along the crystal axes: (a) **a**; (b) **b**; and (c) **c**.

In Figs. 1(a), 1(b), and 1(c) we present the magnetostriction (MS) isotherms for the 2-17 compound crystal. In the notation used for the measured strains, $\lambda(\boldsymbol{\alpha},\boldsymbol{\beta})$, $\boldsymbol{\alpha}$ means the magnetization direction and $\boldsymbol{\beta}$ the strain direction. In Figs. 2(a) and 2(b) are plotted the ones for the 2-14 compound crystal. For 2-14 they are fairly linear, within the experimental error, except for the higher temperatures, as the FMS should increase rapidly when approaching T_c.[1] For 2-17 they show a negative curvature at the lower fields. For 2-17 we plotted such isotherm regions and found a low-field (below about 10 T) contribution as $\sqrt{H_a}$, which suggests suppression of spin-wave excitations (stronger as the temperature increases) by the applied magnetic field, and accordingly with discussion in Sec. I.

The natural way to analyze MS measurements is to obtain the irreducible strains (IS), out of the $\lambda(\boldsymbol{\alpha},\boldsymbol{\beta})$ ones, such as[21]

$$\in^{\alpha,1}(\mathbf{ea}) = \lambda(\mathbf{ea},\mathbf{c}) + \lambda(\mathbf{ea},\mathbf{a}) + \lambda(\mathbf{ea},\mathbf{b}), \tag{2.1}$$

$$\in^{\alpha,2}(\mathbf{ea}) = \frac{1}{\sqrt{3}}\left\{\lambda(\mathbf{ea},\mathbf{c}) - \frac{\lambda(\mathbf{ea},\mathbf{a}) + \lambda(\mathbf{ea},\mathbf{b})}{2}\right\}, \tag{2.2}$$

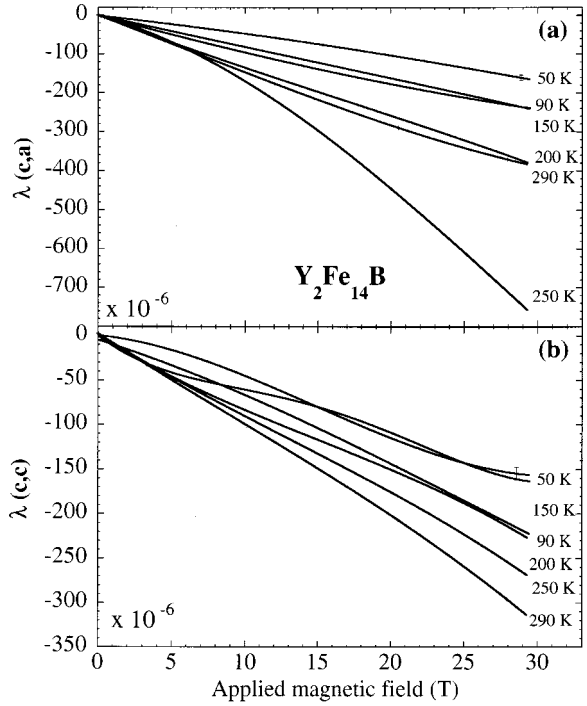

FIG. 2. Magnetostriction isotherms of $Y_2Fe_{14}B$ intermetallic compound for the magnetic field applied along the easy **c** direction, measured along the crystal axes: (a) $\mathbf{a}=\mathbf{b}$ and (b) **c**.

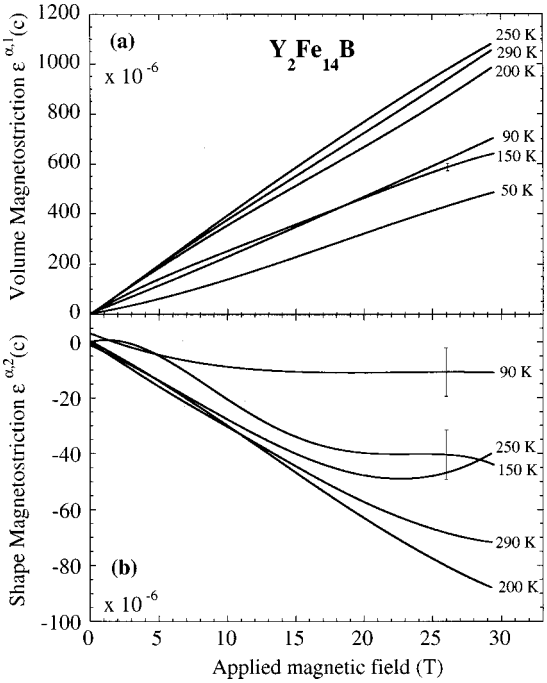

FIG. 4. (a) Selected volume magnetostriction, $\in^{\alpha,1}(\mathbf{c})$, isotherms for applied magnetic field along the easy **c** axis, for a single crystal of $Y_2Fe_{14}B$. (b) The same for shape magnetostriction, $\in^{\alpha,2}(\mathbf{c})$.

where $\mathbf{a}\equiv\mathbf{b}$ for tetragonal symmetry. In Figs. 3(a) and 3(b) we present the strictions $\in^{\alpha,1}(\mathbf{ea})$ and $\in^{\alpha,2}(\mathbf{ea})$ for 2-17 and in Figs. 4(a) and 4(b), the ones for 2-14. The same kind of above comments apply for these isotherms: they show fair linearity with $\mathbf{H_a}$, and lack of perfect linearity likely arises because of error propagation, as we need three $\lambda(\boldsymbol{\alpha},\boldsymbol{\beta})$ strictions measurements to get the IS [Eqs. (2.1) and (2.2)]. The ''anomalous'' behavior of the 150- and 250-K isotherms for $\in^{\alpha,2}(\mathbf{ea})$ for both compounds has been also observed in the rotational or crystal electric-field (CEF) MS $\in^{\alpha,2}(\mathbf{ha})$ (**ha** means hard magnetization axes) at $\cong$200 K, in the form of broad maxima.[22,23] This behavior was explained as the result of transferring $3d$ electrons from nonmagnetostrictive singlet level to a magnetostrictive doublet as temperature increases.[23] The IS's are fairly linear with H_a, with no signs of saturation at 30 T. It is useful to compare the measured IS's with our model calculations below, to define *strain susceptibilities* (SS): $\chi^{\alpha,1}_{\rm mel}(\mathbf{ea})\equiv(\partial\in^{\alpha,1}(\mathbf{ea})/\partial H_a)_T$ and $\chi^{\alpha,2}_{\rm mel}(\mathbf{ea})\equiv(\partial\in^{\alpha,2}(\mathbf{ea})/\partial H_a)_T$, obtained from the slopes of the isotherms of Figs. 3 and 4. In Figs. 5 and 6 we show the

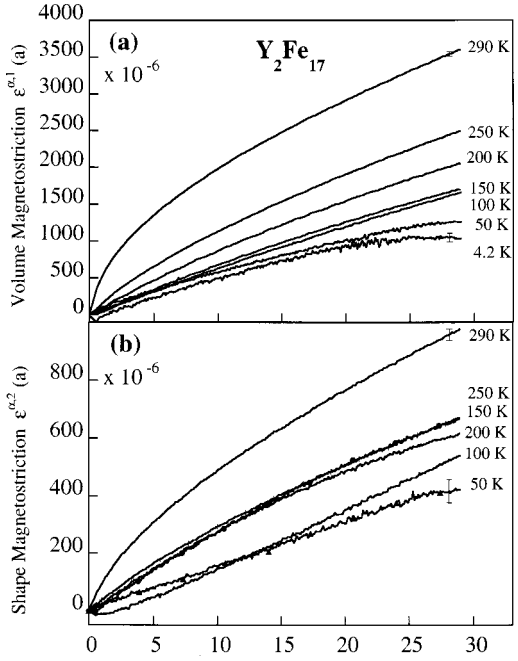

FIG. 3. (a) Selected volume magnetostriction $\in^{\alpha,1}(\mathbf{a})$, isotherms for the applied magnetic field along the easy **a** axis, for a single crystal of Y_2Fe_{17}. (b) The same for shape magnetostriction, $\in^{\alpha,2}(\mathbf{a})$.

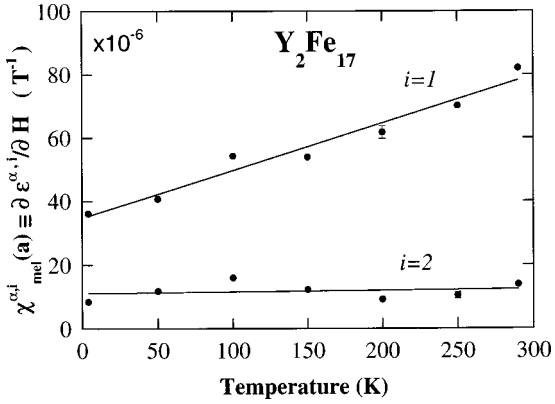

FIG. 5. Thermal variation of the forced magnetostriction susceptibilities, $\chi^{\alpha,i}_{\rm mel}(\mathbf{a})=\partial\in^{\alpha,i}(\mathbf{a})/\partial H$, $i=1$ for volume and $i=2$ for shape, for a Y_2Fe_{17} single crystal. The 30-T magnetic field is applied along the easy **a** axis.

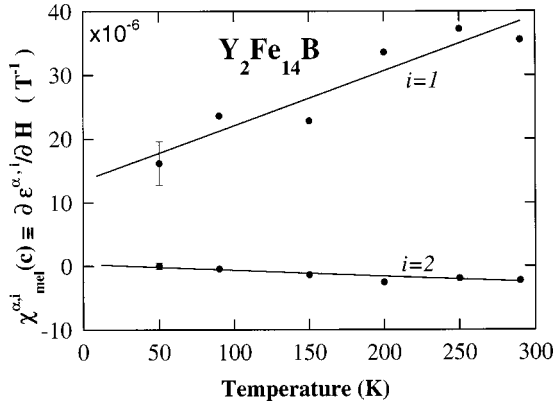

FIG. 6. Thermal variation of the forced magnetostriction susceptibilities, $\chi^{\alpha,i}_{\rm mel}(\mathbf{c})=\partial\epsilon^{\alpha,i}(\mathbf{c})/\partial H$, $i=1$ for volume and $i=2$ for shape, for a $Y_2Fe_{14}B$ single crystal. The 30-T magnetic field is applied along the easy **c** axis.

temperature variations of the SS's for both systems. $\chi^{\alpha,1}_{\rm mel}(\mathbf{ea})$ is about one order of magnitude larger than $\chi^{\alpha,2}_{\rm mel}(\mathbf{ea})$, an unusual feature in $3d$ metals, and both increase with temperature.

Very accurate ''high''-field magnetization isotherms were traced using a superconducting quantum interference device (SQUID) magnetometer up to 5 T and a vibrating sample magnetometer (VSM) up to 12 T. The field up to 30-T magnetization isotherms are shown in Figs. 7(a) and 7(b). $\mathbf{H_a}$ was applied along **ea**. The 5- and 12-T measurements were done in order to guarantee the accuracy of $\chi_{\rm hf}$ as obtained from the 30-T isotherms ($\cong\pm10^{-4}\mu_B$/T Fe atom). From the 5-T and even the 12-T measurements we noticed that $\chi_{\rm hf}$ substantially increased with decreasing magnetic field. The magnetic field range where to obtain the proper $\chi_{\rm hf}$ is a delicate point

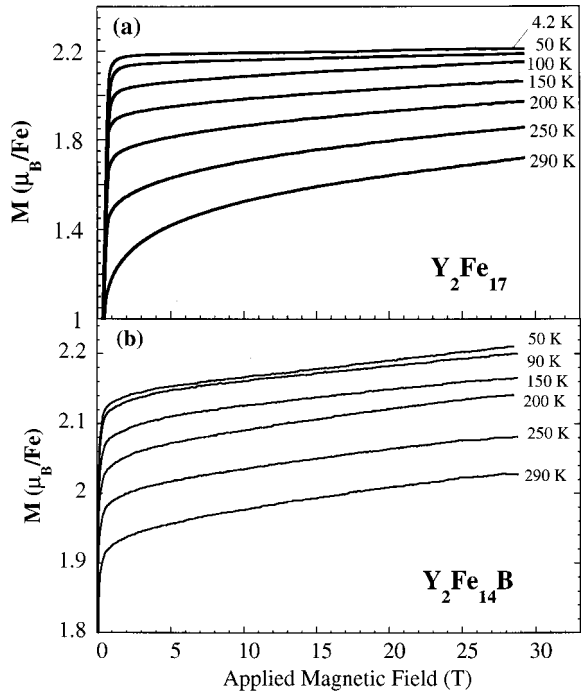

FIG. 7. Forced high-field magnetization (FM) isotherms for: (a) Y_2Fe_{17} and (b) $Y_2Fe_{14}B$ single crystals along the **a** and **c** easy directions, respectively.

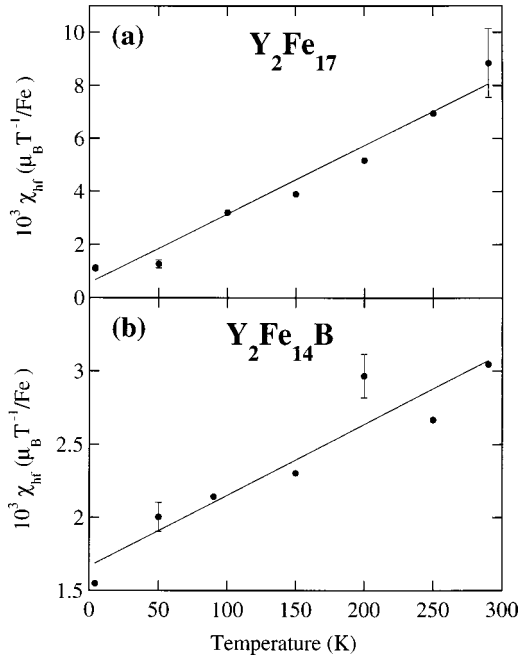

FIG. 8. (a) Thermal variation of the high-field susceptibility along the easy **a** axis, $\chi_{\rm hf}$, for a single crystal of Y_2Fe_{17}. $\chi_{\rm hf}(T)$ is the slope of the isotherm between 15 and 30 T, where magnetization variation is quite linear with applied magnetic field. (b) The same as (a) but for $Y_2Fe_{14}B$ for easy **c** axis.

when dealing with the paraprocess or FM regime. We found as more reliable FM $\chi_{\rm hf}$ values those determined from the magnetization isotherms between 15 and 30 T, where the slopes remain fairly constant [see Figs. 7(a) and 7(b)]. In

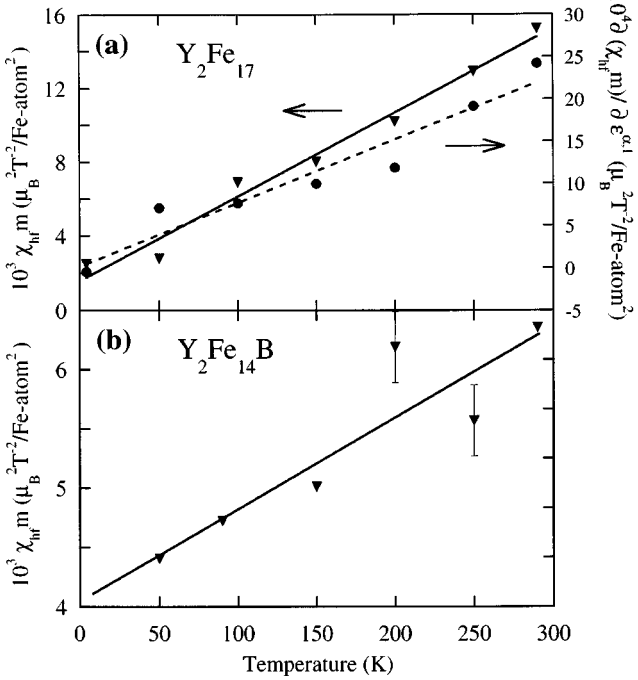

FIG. 9. (a) Thermal variation of the high-field susceptibility times the magnetization $\chi_{\rm hf}m$ against temperature for Y_2Fe_{17} compound along the easy **a** axis (left-hand scale). Also plotted is the derivative against the volume strain $[\partial\chi_{\rm hf}m/\partial\epsilon^{\alpha,1}(\mathbf{a})]_T$. (b) The same as (a) but for $Y_2Fe_{14}B$ compound along the easy **c** axis.

Figs. 8 and 9 we show the thermal variation of the *high-field* susceptibility $\chi_{\rm hf}(T)=(\partial M/\partial H_a)_T$, for 2-17 and 2-14 compounds, respectively, which changes quite linearly with temperature.

III. FORCED MAGNETOSTRICTION (FMS) MODEL

A. Outline of interactions and describing Hamiltonians for Y-Fe intermetallics

We are here mainly interested in showing up the really specific mechanism(s) underlying the high-field FMS. Forced magnetostriction should in principle be contributed by the following mechanisms: (i) magnetic moment rotational fluctuations, both coherent (spin waves) and incoherent (local) against the CEF anisotropy, i.e., single-ion *orbital* contributions to FMS;[22,23] (ii) *two-ion* electron hopping and exchange;[24,25] (iii) *many-body* Coulomb electron repulsion. *Spontaneous* magnetostrictions of kinds (i) and (ii) were extensively studied in those references, and we will only outline them briefly.

Y_2Fe_{17} hexagonal lattice cell contains four unequivalent positions for Fe atoms ($4f$, $6g$, $12j$, $12k$),[9] with our measured site-averaged magnetic moment of $(2.21\pm0.02)\mu_B$/Fe atom and where the ''dumbbell'' of $4f$ atoms supports the highest point symmetry $3m$. For such a symmetry the CEF splitting gives rise to two doublets, $\{|xz\rangle,|yz\rangle\}$, $\{|xy\rangle,|x^2-y^2\rangle\}$ and one singlet, $|2z^2-(x^2+y^2)\rangle$. $Y_2Fe_{14}B$ tetragonal lattice has six unequivalent Fe atom positions,[8] with our measured site-averaged magnetic moment of $(2.20\pm0.02)\mu_B$/Fe atom. As the site point symmetry only supports singlets we early merely assumed[23] an overall tetragonal symmetry for all sites, that gives rise to a doublet $\{|xz\rangle,|yz\rangle\}$ and three singlets. This is the simplest way to get anisotropy and magnetostriction in $Y_2Fe_{14}B$, as observed. More details may be found in Refs. 22 and 23. All single-ion interactions are well described[22,23] by the Hamiltonian

$$H_o=H_{\rm CEF}+H_{\rm so}+H_z+H_{\rm mel}+H_{\rm el}, \tag{3.1}$$

which embodies the following interactions: crystal-field ($H_{\rm CEF}$); spin-orbit ($H_{\rm so}$) one, between the angular momenta $\mathbf{L}$ and $\boldsymbol{\sigma}$; Zeeman (H_z), magnetoelastic ($H_{\rm mel}$), and elastic ($H_{\rm el}$). The particular expressions for these Hamiltonians are not needed here and may be found elsewhere.[22,23] In the Zeeman term is introduced an effective magnetic field, $\mathbf{H}_{\rm eff}=\mathbf{H}_{\rm ex}+\mathbf{H}_a$, where the exchange mean field reads $\mathbf{H}_{\rm ex}=z\mu_B J(\mathbf{r})\langle\boldsymbol{\sigma}\rangle$, with z being the nearest-neighbor (NN) number of Fe atoms for the probe Fe atom; $J(\mathbf{r})$ is the spatially dependent exchange integral and $\langle\boldsymbol{\sigma}\rangle$, the spin thermal average. Those NN's are within the basal planes of the lattice cells. The diagonalization of H_o gives rise to ten energy levels $E^0_{\beta,\pm\sigma}$, where β stands for the orbital state and σ for the spin projection.[22,23] In our previous model[22,23] these levels were the centers of ten energy bands, of width $\Omega_{\beta,\pm\sigma}$, describing the lattice electron energy. All this discussion is needed in order to justify that single-ion CEF magnetostriction could be also present at the FMS process, because of the suppresion of magnetic moment tranversal fluctuations out of the easy axis, by the applied magnetic field. However notice again that only the *orbital* contribution to magnetic moment fluctuations could give rise to crystal-field FMS.

Next sources of FMS should be the two-ion interactions, i.e., electron hopping and exchange. It was shown before[24,25] that in these Y-Fe intermetallics *hopping* between Fe *atom pairs* is a source of spontaneous MS, which is developed below the Curie temperature and it is manifested in the magnetic thermal expansion. This interaction can be described by the simple tight-binding Hubbard Hamiltonian

$$H_h=\sum_{i=1,2}\sum_{\beta,\beta';\sigma} t_{i,3-i;\beta,\beta';\sigma}d^+_{i\beta\sigma}d_{3-i\beta'\sigma}, \tag{3.2}$$

where we demand for having a strain dependence of the $t_{i,3-i;\beta,\beta';\sigma}$ matrix elements. $d^+_{i\beta\sigma}$ and $d_{3-i\beta'\sigma}$ are $3d$-β-band electron creation and annihilation operators, respectively, and i the Fe sites. It was shown before that only the $4f$-$4f$ dumbbell Fe atoms in the case of Y_2Fe_{17} (Ref. 24) and the *e*-*e* pair ones for $Y_2Fe_{14}B$ (Ref. 25) are involved in the two-ion magnetostriction (both pairs are along the main **c**-crystal axis). The reason is that, by symmetry considerations and because of orbital overlapping, only t-matrix elements for electron hopping between those pairs are not zero *and* preserve the magnetostrictive $\{|xz\rangle,|yz\rangle\}$ doublets.[24,25] However, strain dependent exchange interaction $J(\mathbf{r})$, was also shown to be a source of MS.[24,25] Diagonalization of H_h produces a further splitting of the energy levels, 20 overall, with energies $E^0_{\beta,\pm\sigma,t,J}$, which become again the centers of correspondingly 20 $3d$ bands. Strain dependencies of $E^0_{\beta,\pm\sigma,t,J}$ levels are the sources of one-ion and two-ion FMS's.

Summarizing until now, the MEL coupling distorts the CEF bringing about the single-ion magnetostriction eventually contributing to the FMS, because of transversal magnetic-moment fluctuations. The t matrix is Fe-Fe distance dependent, as well as the $J(\mathbf{r})$ exchange of the magnetostrictive Fe pair with NN, and both give rise to FMS of two-ion origin. In fact, as mentioned before, *spontaneous* or coherent magnetostriction from these two sources were already observed in Y_2Fe_{17} and $Y_2Fe_{14}B$ compounds and thoroughly studied there.[22–25] The single-ion spontaneous CEF magnetostriction appears when the magnetization rotates away from the **ea**. The two-ion or electron hopping one should be significant because of the large strains observed in the FMS, of about the same order of magnitude than the spontaneous magnetic thermal expansion below T_C [at 250 K $\in^{\alpha,1}(\mathbf{ea})\cong 7.7\times10^{-3}$ and 19×10^{-3}, for 2-17 and 2-14 respectively].[24,25] Therefore at the FMS process both strictions should be eventually present.

B. Many-body Hubbard magnetostriction

We come about to the main FMS specific source, in which we are interested to reveal for these Y-Fe intermetallics, as it is the $3d$-electron *Coulomb* interaction. Physically $3d$-electron Coulomb repulsion energy should be another source of FMS as it is interelectronic distance dependent (i.e., strain dependent) and, in principle, rather strong. We will show that this *many-body* interaction is the main source of FMS for the present iron rich intermetallics. The assumed Hamiltonian describing $3d$ electron many-body interactions is the simplest Hubbard one,

$$H_{\rm mb}=\sum_{i;\beta,\beta';t\text{-}J} U^{\rm eff}_{\beta,\beta'} n_{i,\beta,t\text{-}J,\sigma} n_{i,\beta',t\text{-}J,-\sigma}. \quad (3.3)$$

In Eq. (3.3), $U^{\rm eff}_{\beta,\beta'}$ is the *effective* electron Coulomb repulsion, i the Fe site, β the $3d$ band orbital state, t-J the index for two-ion interaction, σ ($=\pm\frac{1}{2}$), the spin projection along the easy axis, and $n_{i,\beta,t\text{-}J,\sigma}$ the electron number operator. Coulomb repulsion between $3d$ electrons will be source of FMS, if we assume the $U^{\rm eff}_{\beta,\beta'}$ potential to be *strain dependent*. In other words we assume that many-body effects are responsible as well for the FMS. In Eq. (3.3) we should consider two effective $U^{\rm eff}_{\beta,\beta'}$ potentials: when $\beta=\beta'$ (intraband electron repulsion) and $\beta\neq\beta'$ (interband electron repulsion), with potentials U_n and U_d, respectively, and $U_d > U_n$, because band formation increases energy (we drop off the ''eff'' superscript in $U^{\rm eff}_n$ and $U^{\rm eff}_d$ for simplicity in notation). We now treat $H_{\rm mb}$ within the Hartree-Fock approximation, i.e., neglecting charge and *spin* thermal fluctuations.[3,14] However, orbital magnetic-moment fluctuations are introduced in our model in the sense discussed in Sec. III A. Then we obtain $\overline{n}_\gamma=\langle n_{\gamma\sigma}\rangle+\langle n_{\gamma-\sigma}\rangle$ and $\overline{m}_\gamma/\mu_B=\langle n_{\gamma\sigma}\rangle-\langle n_{\gamma-\sigma}\rangle$, as the thermal averages of the γ-band electron population and magnetization, respectively. To simplify notation, γ now stands for the β, t, J, and U indices in the energy levels. These levels are readily obtained as (per Fe atom),

$$E_{\gamma,\pm\sigma}=E^0_{\beta,\pm\sigma}+E^0_{t\text{-}J}-\frac{U_n}{4}(\pm m-n)+\frac{U_d}{2}(n-\overline{n}_\gamma), \quad (3.4)$$

where $n=\Sigma_{\gamma,\pm\sigma}\langle n_{\gamma,\pm\sigma}\rangle$ is the equilibrium number of electrons within the 20 subbands and m the magnetization (in μ_B) (both per Fe atom).

Under the assumption of rigid γ-band shifts, $\Delta E_{i,\gamma,\pm\sigma}$, under applied magnetic field and strain distortion, the gain in magnetic free energy F_m is[22]

$$\Delta F_m=-\sum_{i,\gamma,\pm\sigma}\langle n_{i,\gamma,\pm\sigma}\rangle\Delta E_{i,\gamma,\pm\sigma}. \quad (3.5)$$

In order to get the equilibrium strictions we have to minimize $F_m+F_{\rm el}$ against the irreducible strains, where $F_{\rm el}$ is the elastic energy, which is given in Refs. 1 and 20. We have two kinds of $\partial F_m/\partial\in^{\alpha,1}$ terms: one related to the strain dependence of the levels $E^0_{\gamma,\pm\sigma}=E^0_{\beta,\pm\sigma}+E^0_{t\text{-}J}$ and the remaining terms related to Coulomb U interactions [Eq. (3.4)]. The system of equations so derived is readily obtained in the form (per Fe atom)

$$\begin{aligned}-\sum_{\gamma,\pm\sigma}\langle\overline{n}_{\gamma,\pm\sigma}\rangle\partial E^0_{\gamma,\pm\sigma}/\partial\in^{\alpha,i}&+(U_n/8)\partial m^2/\partial\in^{\alpha,i}\\&+(U_d/4)\sum_\gamma\partial(\overline{n}^2_\gamma)/\partial\in^{\alpha,i}\\&+(m^2/2)(\partial U_n/\partial\in^{\alpha,i})+(1/2)\\&\times(\partial U_d/\partial\in^{\alpha,1})\left(\sum_\gamma\overline{n}^2_\gamma-n^2\right)\\&+C^\alpha_{i1}\in^{\alpha,1}+C^\alpha_{i2}\in^{\alpha,2}=0, \quad (3.6)\end{aligned}$$

with $i=1,2$, and where C^α_{ij} are the symmetry elastic stiffness constants.[1,20] It is now more convenient to work with the SS's above defined. Therefore we proceed to take the derivative of Eq. (3.6) against the applied magnetic field H_a and obtain a system of equations in the SS's. Details of the calculations are included in Appendix A, where we discuss the approximations and simplifications introduced in our calculations in order to arrive at the following leading terms for the SS's:

$$\begin{aligned}\chi^{\alpha,i}_{\rm mel}=\chi^{\alpha,i}_{\rm mel,0}-\frac{1}{C^\alpha_{ii}}\Bigg\{&\left(\frac{\partial U^{\rm eff}_n}{\partial\in^{\alpha,i}}\right)_T\chi_{\rm hf}(T)m(T)\\&+\frac{U^{\rm eff}_n}{4}\left(\frac{\partial}{\partial\in^{\alpha,i}}[\chi_{\rm hf}(T)m(T)]\right)_T\Bigg\}, \quad i=1,2, \quad (3.7)\end{aligned}$$

where $\chi^{\alpha,i}_{\rm mel,0}$ are the susceptibilities resulting from the single-ion CEF, hopping and interatomic exchange mechanisms. As we can see, two mechanisms are in principle contributing to the FMS, although both bear upon the many-body electron Coulomb interaction. The second term in Eq. (3.7) gives the contribution from the strain dependence of *intraband* Coulomb potential and third one accounts for the strain dependence of magnetization. The prediction from Eq. (3.7) is the linear dependence of the SS's with the product $\chi_{\rm hf}(T)m(T)$ and with $[\partial\chi_{\rm hf}(T)m(T)/\partial\in^{\alpha,i}]_T$. First linear dependence keeps remarkably well with Wohlfarth's phenomenological relation (1.1) and even a second one also appears in Wohlfarth's relation if one considers m to be strain dependent. The kind of agreement achieved gives further credit to our model Eq. (3.7).

IV. COMPARISON WITH EXPERIMENT AND RESULTS

A. Obtainment of $U^{\rm eff}$ and $\partial U^{\rm eff}/\partial\in^{\alpha,i}$ parameters

Model Eq. (3.7) suggests plotting the experimental SS's $\chi^{\alpha,1}_{\rm mel}$ and $\chi^{\alpha,2}_{\rm mel}$ values against the product $\chi_{\rm hf}(T)m(T)$ on one side and on the other side against $[\partial\chi_{\rm hf}(T)m(T)/\partial\in^{\alpha,i}]_T$. In Figs. 9(a) and 9(b) we show the thermal variation of $\chi_{\rm hf}(T)m(T)$ for 2-17 and 2-14 compounds, respectively. This linear dependence with temperature keeps well with the observed ones for $\chi^{\alpha,1}_{\rm mel}$ and $\chi^{\alpha,2}_{\rm mel}$ (see Figs. 5 and 6), as model Eq. (3.7) predicts. In the case of Y_2Fe_{17} compound there also exist measurements on the pressure dependence of $m(T)$ and $\chi_{\rm hf}(T)$,[26] and in Fig. 9(a) we have plotted the thermal dependence of $[\partial\chi_{\rm hf}(T)m(T)/\partial\in^{\alpha,i}]_T$, which changes linearly with temperature, in agreement with Eq. (3.7) prediction. In Figs. 10(a) and 11 we show the plots of SS's $\chi^{\alpha,i}_{\rm mel}$(**ea**) against $\chi_{\rm hf}(T)m(T)$ for 2-17 and 2-14 compounds, respectively, and in Fig. 10(b) the plots against $[\partial\chi_{\rm hf}(T)m(T)/\partial\in^{\alpha,i}]_T$ for 2-17 compound. We can see that Eq. (3.7) predicted *separate* linearities are rather well accomplished for both compounds. These plots suggest that effectively it is the many-body $3d$-electron interaction U_n and its strain dependence $\partial U_n/\partial\in^{\alpha,i}$, the specific and basic mechanisms underlying the FMS in our Fe-rich intermetallics.

A fully consistent determination of $U^{\rm eff}_n$ and $\partial U^{\rm eff}_n/\partial\in^{\alpha,i}$ from our experimental results is rather difficult, considering that $\chi^{\alpha,i}_{\rm mel,0}$ strains are unknown too and their theoretical calculation would give quite uncertain values. Instead, from

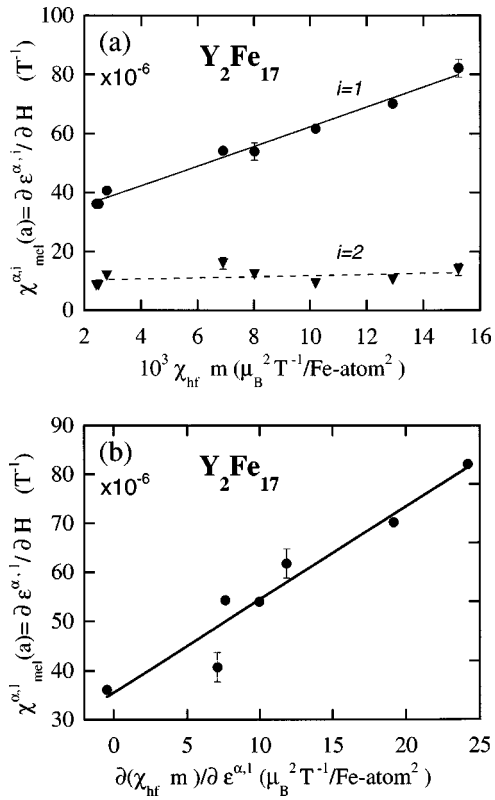

FIG. 10. (a) Plots of the forced magnetostriction susceptibilities $[\partial \in^{\alpha,i}(\mathbf{a})/\partial H]_T$ of volume $(i=1)$ and shape $(i=2)$ against the product $\chi_{\rm hf}(T)m(T)$, as suggested by model Eq. (3.7), for Y_2Fe_{17} compound. The straight lines are the ''best'' fit ones. The intercepts on the vertical axis are $\chi^{\alpha,i}_{\rm mel,0}(\mathbf{a})$. (b) The same as (a) but now $[\partial \in^{\alpha,1}(\mathbf{a})/\partial H]_T$ against $[\partial \chi_{\rm hf} m/\partial \in^{\alpha,1}(\mathbf{a})]_T$, as Eq. (3.7) also suggests.

Figs. 10(a) and 11 plots we can estimate, from the vertical axis intercepts, the contribution to the SS's from CEF and two-ion interactions $\chi^{\alpha,i}_{\rm mel,0}$ and from the line slopes $\partial U_n^{\rm eff}/\partial \in^{\alpha,i}$. The values so obtained are quoted in Table I. For such an obtainment, we took for the elastic stiffness constants the estimated values for $Y_2Fe_{14}B$, $C^{\alpha}_{11} \cong 12.5$ eV/Fe atom and $C^{\alpha}_{22} \cong 30$ eV/Fe atom.[23] Values for C^{α}_{ii} for Y_2Fe_{17} are not available. Therefore, the strain dependence of $3d$-electron effective Coulomb potential can be determined from FMS and FM experiments in $3d$ ferromagnetic metals and alloys.

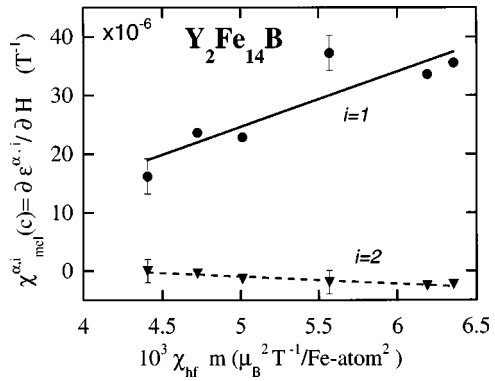

FIG. 11. The same as Fig. 10(a) but for $Y_2Fe_{14}B$ intermetallic compound; now the magnitudes refer to the easy **c** axis.

TABLE I. Strain susceptibilities $\chi^{\alpha,i}_{\rm mel,0}$ in units of $10^{-6}\,{\rm T}^{-1}$, and strain derivatives $\partial U_n^{\rm eff}/\partial \in^{\alpha,i}$ in units of eV Fe atom, obtained for the Y_2Fe_{17} and $Y_2Fe_{14}B$ intermetallics (see main text for their meanings).

Compound	$\chi^{\alpha,1}_{\rm mel,0}$	$\chi^{\alpha,2}_{\rm mel,0}$	$-(\partial U_n^{\rm eff}/\partial \in^{\alpha,1})$	$-(\partial U_n^{\rm eff}/\partial \in^{\alpha,2})$
Y_2Fe_{17}	35	10	0.04 ± 0.002	$0.006 \pm 3 \times 10^{-4}$
$Y_2Fe_{14}B$	10	$\cong 0$	0.12 ± 0.05	-0.04 ± 0.01

On the other side from the slopes of Fig. 11 we determined a zero-strain value $U_n^{\rm eff} \cong 1$ meV/Fe atom for Y_2Fe_{17}. This value is too small compared with the accepted one for Fe metal of ≈ 1 eV.[2,3] This result is rather surprising and we will discuss it in Sec. V below.

B. Strain dependence of bandwidths

For doing our model calculation of the SS's, we introduced in our Hubbard Hamiltonian [see Eq. (3.3)] effective Coulomb potentials which become strain dependent, as shown in Sec. III B. However, this strain dependence goes beyond the simplest Hubbard U potential which is assumed to be an ''on-site'' one.[3,14] To find an explanation of how the $U_n^{\rm eff}$ intraband potential can become strain dependent is a major problem within our model. However, we allow for electron hopping between Fe atom pairs [see Eq. (3.2)] and therefore the ''bare'' U_n^0 potential is strongly renormalized by hopping by a factor $-4\langle|t|\rangle^2/[U_n^0]^2$, for small enough $\langle|t|\rangle/U_n^0$, where the symbols $\langle|t|\rangle$ stand for the relevant t_0-matrix elements. The detailed calculation of this particular reduction of U_n^0 is beyond the scope of this work and will be discussed in future work.

On the other side, if we consider electron-electron scattering, we should replace the ''bare'' U_n^0 potential by the *effective* one,[3,6] $U_n^{\rm eff} \cong U_n^0/(1+FU_n^0)$, where $F \approx c/\Omega$, with Ω being the $3d$-band width. Then if the rigid band approximation is abandoned, it is straightforward to show that

$$\frac{\partial \Omega}{\partial \in^{\alpha,i}} \cong \frac{1}{c}\left(\frac{\Omega}{U_n^{\rm eff}}\right)^2\left(\frac{\partial U_n^{\rm eff}}{\partial \in^{\alpha,i}}\right). \tag{4.1}$$

However, notice that our model, because of the different shifts introduced in the individual γ $3d$ bands by applied field or strain, takes already into account to some extent a nonrigid electronic structure band density of states.[22–25] The disposable value for iron metal is $U_n^0/\Omega \cong 0.1$ (Refs. 3, 6, and 14) and $c \approx 1$.[6,14] The calculated[28–30] $3d$ and overall (i.e., considering $3d$-$4s$ band hybridization) bandwidth values are

TABLE II. Calculated (Refs. 28–30) $3d$-band widths ($3d$-BW) and hybridized bandwidths (H-BW) and their presently estimated strain dependencies for Y_2Fe_{17} and $Y_2Fe_{14}B$ intermetallics (see details in the main text about their obtainment).

Compound	Bandwidth (eV)		$-(\partial \ln \Omega/\partial \in^{\alpha,1})$		$-(\partial \ln \Omega/\partial \in^{\alpha,2})$	
	$3d$-BW	H-BW	H-BW	$3d$-BW	H-BW	$3d$-BW
Y_2Fe_{17}	4.8	7	0.6	0.9	0.085	0.1
$Y_2Fe_{14}B$	5.8	6.1	1.3	2.0	-0.4	-0.6

displayed in Table II. In these calculations[28–30] $3d$-electron correlation was introduced. Also in Table II are our estimated strain dependencies of the bandwidths, from Eq. (4.1) and using the values of Table I. The accepted Heine's theoretical value[31] of the Ω volume logarithmic derivative is $-\frac{5}{3}$, in reasonable agreement with the values quoted in Table II, if we consider the spread in values existent for U_n^0.[2,3,14] However, these estimates would need to be checked experimentally in a more direct manner, e.g., by electron photoemission under stress, for our 2-14 and 2-17 intermetallics.

V. DISCUSSION AND CONCLUSIONS

The value found for the effective Coulomb potential $U_n^{\rm eff}$ is clearly too small. This result is rather puzzling if we consider the good linearity found for the SS's against $[\partial\chi_{\rm hf}(T)m(T)/\partial\in^{\alpha,i}]_T$ (Fig. 11), as our model Eq. (3.7) predicts and the convincing values found for its derivatives $\partial U_n^{\rm eff}/\partial\in^{\alpha,i}$. We do not have presently any fully definitive argument for giving an explanation of such a small value. A possibility, as we mentioned before, is if the $U_n^{\rm eff}$ value here obtained were the result of a renormalization of U_n^0 by a factor $\cong(-4\langle|t|\rangle^2/[U_n^0]^2+J/U_n^0)$, where $J^{\rm eff}>0$ is the effective exchange interaction integral.[27] This reduction will be the subject of future theoretical work.

Now we should discuss the terms disregarded within our simple Coulomb interaction Hamiltonian of Eq. (3.3), $H_{\rm mb}$. There we did not consider $3d$-electron *exchange* interaction between the Fe pair atoms, that amounts for an extra term (per Fe site) of the form[3,27]

$$H_{\rm ex}=(U_d^{\rm eff}-J_d^{\rm eff})\sum_{\beta\neq\beta';t\text{-}J;\sigma} n_{\beta,t\text{-}J,\sigma}n_{\beta',t\text{-}J,\sigma}, \qquad (5.1)$$

where $J_d^{\rm eff}$ is the exchange effective potential, assumed to be the same for all β bands. In Appendix B we treat $H_{\rm ex}$ within the Hartree-Fock approximation, and find that the effective exchange interaction of the pair atoms does not contribute to the FMS strain susceptibilities, within our model.

Another point for discussion is how the parameters $U_n^{\rm eff}$ and $\partial U_n^{\rm eff}/\partial\in^{\alpha,i}$ have been obtained. Model Eq. (3.7) is a plane in the threefold Cartesian spaces, $z\equiv\chi_{\rm mel}^{\alpha,i}$, $x\equiv\chi_{\rm hf}(T)m(T)$, and $y\equiv[\partial\chi_{\rm hf}(T)m(T)/\partial\in^{\alpha,i}]_T$, $i=1,2$, which cut the Cartesian planes (z,x) and (z,y) along straight lines, as in fact it is experimentally observed. Therefore a fully consistent determination of those parameters should be found by fitting the experimental results within the $Ax+By+z-z_0=0$ plane and getting the A, B, and z_0 parameters together ($z_0\equiv\chi_{\rm mel,0}^{\alpha,i}$). However, this fitting procedure turned out to be quite difficult and unsuccessful, with the disposable experimental results at hand, and we did not find triplets (z_0,A,B) with more sound physical meaning. Nevertheless, the good linear fits found by projecting Eqs. (3.7) on the Cartesian planes and the sound values of $\partial U_n^{\rm eff}/\partial\in^{\alpha,i}$ are both rather satisfying.

On the other hand, the α-mode decoupling practiced with the volume $\in^{\alpha,i}$ and shape $\in^{\alpha,2}$ forced magnetostrictions seems quite realistic on the sight of the general good agreement found between experiment and model calculations.

To conclude, we have shown that the temperature dependencies of the strain susceptibilities of volume $[\partial\in^{\alpha,1}(\mathbf{ea})/\partial H]_T$ and shape $[\partial\in^{\alpha,2}(\mathbf{ea})/\partial H]_T$ for the Fe-rich uniaxial intermetallics Y_2Fe_{17} and $Y_2Fe_{14}B$ can be rather well explained by a simple Hubbard-like model, assuming that the *effective* $3d$ intraband Coulomb potential $U_n^{\rm eff}$ is strain dependent. Apparently reasonable values for the strain derivatives of the effective Coulomb potential have been obtained. Our findings show how good forced magnetostriction is in probing many-body electron effects in $3d$ metals. Possible origins for these strain dependencies have been briefly discussed, in particular the dependence on the band electronic structure. Contributions of Fe atom volume and shape distortions produced by the forced strictions seem to be substantial. Overall our model looks quite successful in explaining forced magnetostriction in the above intermetallic compounds. We hope that our findings could stimulate further experiments and more sophisticated models for checking the appearance of *many-electron* effects in the forced magnetostriction of Fe-rich alloys and intermetallics.

ACKNOWLDGMENTS

We are grateful to Professor J. J. M. Franse and to Professor D. Givord for the single-crystal provision, to Dr. K. Kulakowski for useful discussions and comments, to Engineer M. Hilbers and Dr. P. A. Algarabel for assistance with the high magnetic-field experiments, and to Dr. Z. Arnold for high-pressure results. We acknowledge the Spanish CICYT for financial assistance under Project No. MAT97/1038.

APPENDIX A

In order to solve the system of Eqs. (3.4) we will make the definitions (for index $i=1,2$):

$$\begin{aligned}-O_i\equiv{}&(U_n/8)[\partial m^2/\partial\in^{\alpha,i}]+(U_d/4)\sum_\gamma \partial(\overline{n}_\gamma^2)/\partial\in^{\alpha,i}\\&+(m^2/2)(\partial U_n/\partial\in^{\alpha,i})\\&+(1/2)(\partial U_d/\in^{\alpha,i})\left(\sum_\gamma \overline{n}_\gamma^2-n^2\right).\end{aligned} \qquad (A1)$$

Then from Eq. (3.4) we obtain the system of two linear equations for the equilibrium strictions,

$$C_{i1}^\alpha\in^{\alpha,1}+C_{i2}^\alpha\in^{\alpha,2}=\sum_{\gamma,\pm\sigma}\langle n_{\gamma,\pm\sigma}\rangle\partial E^0_{\gamma,\pm\sigma}/\partial\in^{\alpha,i}+O_i. \qquad (A2)$$

It is far more convenient to work with SS's than with strains themselves and therefore we take the derivative of Eqs. (A2) against the applied magnetic field H_a. We found

$$\begin{aligned}\chi_{\rm mel}^{\alpha,1}&=\chi_{\rm mel,0}^{\alpha,1}+\frac{1}{\Delta^\beta}\left(C_{22}^\alpha\frac{\partial O_1}{\partial H_a}-C_{12}^\alpha\frac{\partial O_2}{\partial H_a}\right),\\ \chi_{\rm mel}^{\alpha,2}&=\chi_{\rm mel,0}^{\alpha,2}+\frac{1}{\Delta^\beta}\left(C_{11}^\alpha\frac{\partial O_2}{\partial H_a}-C_{12}^\alpha\frac{\partial O_1}{\partial H_a}\right),\end{aligned} \qquad (A3)$$

where $\Delta^\alpha=C_{11}^\alpha C_{22}^\alpha-(C_{12}^\alpha)^2$ and $\chi_{\rm mel,0}^{\alpha,i}$ are the SS's coming from the strain dependence of CEF, two-ion, and *NN* ex-

change energy levels and which their expressions are obtained just substituting in Eqs. (A3) O_i by $\Sigma_{\gamma,\pm\sigma}\langle n_{\gamma,\pm\sigma}\rangle \partial E^0_{\gamma,\pm\sigma}/\partial \in^{\alpha,i}$. We are now going to assume that the order of the partial derivatives of O_i against strains $\in^{\alpha,i}$ and field H_a can be interchanged. This is not strictly true because the strictions depend on H_a. However, we know from experiment[26] that the order of derivatives is irrelevant in the case of the magnetization m and it is reasonable to extend such an assumption to the derivatives of the occupation numbers $\overline{n}_\gamma$. From Eq. (A1) we immediately obtain

$$-\frac{\partial O_i}{\partial H_a}=\left(\frac{\partial U_n}{\partial \in^{\alpha,i}}\right)\chi_{\rm hf}m+\left(\frac{U_n}{4}\right)\frac{\partial(\chi_{\rm hf}m)}{\partial \in^{\alpha,i}}+\left(\frac{U_d}{4}\right)\frac{\partial}{\partial \in^{\alpha,i}}\sum_\gamma \frac{\partial \overline{n}^2_\gamma}{\partial H_a}+\left(\frac{1}{2}\frac{\partial U_d}{\partial \in^{\alpha,i}}\right)\sum_\gamma \frac{\partial \overline{n}^2_\gamma}{\partial H_a}. \tag{A4}$$

We will now show that for weakly spin-dependent band density of states, which is the actual situation for our 2-14 and 2-17 intermetallics according to polarized band-structure calculations,[28–30] $\Sigma_\gamma \partial \overline{n}^2_\gamma/\partial H_a$ is small and therefore we can neglect terms in U_d and $(\partial U_d/\partial \in^{\alpha,i})$ in Eq. (A4). The γ-band number of electrons is

$$\overline{n}_\gamma=\int_{-\infty}^{\mu}\{\rho_{\gamma,+\sigma}(E-E_{\gamma,+\sigma})+\rho_{\gamma,-\sigma}(E-E_{\gamma,-\sigma})\}dE, \tag{A5}$$

where $\rho_{\gamma,\pm\sigma}$ are the functions density of states for the two spin projections and μ the chemical potential. Now if we assume that $\partial\rho_{\gamma,+\sigma}/\partial E_{\gamma,+\sigma}\cong\partial\rho_{\gamma,-\sigma}/\partial E_{\gamma,-\sigma}\equiv\partial\rho_\gamma/\partial E_{\gamma,|\sigma|}$ and take the derivative of $\overline{n}_\gamma$ against H_a, using Eq. (A5) we obtain

$$\frac{1}{2}\sum_\gamma \frac{\partial \overline{n}^2_\gamma}{\partial H_a}=\sum_\gamma \overline{n}_\gamma\int_{-\infty}^{\mu}\frac{\partial\rho_\gamma}{\partial E_{\gamma,|\sigma|}}\left(\frac{\partial E_{\gamma,+\sigma}}{\partial H_a}+\frac{\partial E_{\gamma,-\sigma}}{\partial H_a}\right)dE. \tag{A6}$$

Now from Eq. (3.4) it is easily shown that

$$\frac{\partial E_{\gamma,+\sigma}}{\partial H_a}+\frac{\partial E_{\gamma,-\sigma}}{\partial H_a}=-U_d\frac{\partial \overline{n}_\gamma}{\partial H_a}, \tag{A7}$$

and plugging Eq. (A7) into Eq. (A6) one finally arrives at the expression

$$\frac{\partial \overline{n}_\gamma}{\partial H_a}\left(1+U_d\int_{-\infty}^{\mu}\frac{\partial\rho_\gamma}{\partial E_{\gamma,|\sigma|}}dE\right)=0, \tag{A8}$$

and because the parameter U_d is, in principle, arbitrary we see that $\partial\overline{n}_\gamma/\partial H_a\cong 0$ and therefore $\Sigma_\gamma(\partial\overline{n}^2_\gamma/\partial H_a)\cong 0$. If we introduce this result in Eq. (A4) we effectively remove terms depending on the interband Coulomb potential U_d. This result obviously means that spin-down transfer to spin up under Zeeman polarization occurs for each γ band separately.

Finally, in order to solve the linear system of Eqs. (A3) we have decoupled the two α strains. This procedure is equivalent to assume C^α_{12} small, a reasonable approximation.[22,23] With such a procedure we can arrive at Eq. (3.5), as shown in Sec. III.

APPENDIX B

We treat $H_{\rm ex}$ of Eq. (5.1) within the Hartree-Fock approximation and, in a first-order perturbation, we readily obtain

$$E_{\rm ex}=(U^{\rm eff}_d-J^{\rm eff}_d)\sum_{\beta\neq\beta'}(\overline{n}_\gamma+\overline{n}'_\gamma), \tag{B1}$$

energy that will be added to the energy levels of Eq. (3.4). When introducing Eq. (B1) in Eq. (3.5) we obtain

$$-\frac{\partial F^{\rm ex}_m}{\partial \in^{\alpha,i}}=(U^{\rm eff}_d-J^{\rm eff}_d)\sum_{\rho,\gamma\neq\gamma'}\overline{n}_\rho\frac{\partial(\overline{n}_\gamma+\overline{n}'_\gamma)}{\partial \in^{\alpha,i}}+\frac{\partial(U^{\rm eff}_d-J^{\rm eff}_d)}{\partial \in^{\alpha,i}}\sum_{\rho,\gamma\neq\gamma'}\overline{n}_\rho(\overline{n}_\gamma+\overline{n}'_\gamma). \tag{B2}$$

Now term (B2) is added to the right-hand side of Eq. (A2) and when performing the derivative of Eqs. (B2) against H_a, as done before, these terms become null as $\partial\overline{n}_\delta/\partial H_a=0$, for $\delta=\gamma,\gamma',\rho$.

[1] E. W. Lee, Rep. Prog. Phys. **18**, 184 (1955); E. T. de Lacheisserie, *Magnetostriction* (CRC, Boca Raton, 1993); W. J. Carr, in *Handbuch der Physik*, edited by S. Flüge (Springer-Verlag, Berlin, 1966), p. 274; A. del Moral and M. R. Ibarra, *Magnetostriction: Basic Principles and Materials* (Adam-Hilger & Institute of Physics, London, in Press).

[2] E. P. Wohlfarth, in *Ferromagnetic Materials* (North-Holland, Amsterdam, 1980), Vol. 1, p. 1.

[3] F. Gautier, in *Magnetism of Metals and Alloys*, edited by M. Cyrot (North-Holland, Amsterdam, 1982), p. 1.

[4] R. Pauthenet, in *High Field Magnetism*, edited by M. Date (North-Holland, Amsterdam, 1983), p. 71.

[5] E. F. Wasserman, in *Ferromagnetic Materials*, edited by K. H. J. Buschow and E. P. Wohlfarth (North-Holland, Amsterdam, 1990), Vol. 5, p. 271.

[6] J. Kanamori, Prog. Theor. Phys. **30**, 275 (1963); C. Herring, in *Magnetism*, edited by G. T. Rado and H. Suhl (Academic, New York, 1965), Vol. II.B.

[7] J. M. H. Stoelinga, R. Gersdorf, and G. de Vries, Physica (Amsterdam) **31**, 349 (1965); G. M. Williams and A. S. Pavlovic, J. Appl. Phys. **39**, 571 (1968); E. W. Lee and M. A. Asgar, Proc. R. Soc. London, Ser. A **326**, 73 (1971).

[8] J. F. Herbst, Rev. Mod. Phys. **63**, 819 (1991).

[9] D. Givord, R. Lemaire, J. M. Moreau, and E. Roudaut, J. Less-Common Met. **29**, 361 (1972).

[10] T. Holstein and H. Primakoff, Phys. Rev. **58**, 1098 (1940).

[11] A. del Moral and M. S. S. Brooks, J. Phys. C **7**, 2540 (1974).

[12] K. Ried, V. Özpamir, and H. Kronmüller, Phys. Rev. B **50**, 10 027 (1994), and references therein.

[13] H. M. Mayer, M. Steiner, N. Stüsser, H. Weinfurter, B. Dorner, P. A. Lingard, K. N. Clausen, S. Hock, and R. Verhoef, J. Magn. Magn. Mater. **104-107**, 1295 (1992).
[14] D. Wagner, *Introduction to the Theory of Magnetism* (Pergamon, New York, 1972); R. M. White, *Quantum Theory of Magnetism* (McGraw-Hill, New York, 1970).
[15] E. P. Wohlfarth, J. Phys. C **2**, 68 (1969).
[16] A. Katsuki and T. Terao, J. Phys. Soc. Jpn. **26**, 1109 (1969); **27**, 321 (1969).
[17] F. Herlach and Jos A. J. J. Peremboom, Physica B **211**, 1 (1995).
[18] E. W. Lee, in *Experimental Magnetism*, edited by G. M. Kalvius and R. S. Tebble (Wiley, New York, 1979), Vol. 1, p. 226.
[19] A. del Moral and D. Melville, An. Fís. (Madrid) **70**, 219 (1974).
[20] E. R. Callen and H. B. Callen, Phys. Rev. **129**, 578 (1963); Phys. Rev. **139**, A455 (1965).
[21] A. del Moral, M. R. Ibarra, P. A. Algarabel, and J. I. Arnaudas, in *Physics of Magnetic Materials*, edited by W. Gorzkowski, M. Gutowski, H. K. Lachowicz, and H. Szymczak (World Scientific, Singapore, 1991), p. 90; A. del Moral, in *Magnetoelastic Effects and Applications*, edited by L. Lanotte (Kluwer, Amsterdam, 1993), p. 1, and references therein.
[22] K. Kulakowski and A. del Moral, Phys. Rev. B **50**, 234 (1994).
[23] C. Abadía, A. del Moral, K. Kulakowski, and P. A. Algarabel, J. Phys.: Condens. Matter **11**, 3341 (1999).
[24] K. Kulakowski and A. del Moral, Phys. Rev. B **52**, 15 943 (1995).
[25] C. Abadía, A. del Moral, K. Kulakowski, and P. A. Algarabel, Phys. Rev. B **59**, 486 (1999).
[26] J. Kamarád, O. Mikulina, Z. Arnold, B. García-Landa, and M. R. Ibarra, J. Appl. Phys. **85**, 4874 (1999); O. Mikulina, J. Kamarád, Z. Arnold, B. García-Landa, P. A. Algarabel, and M. R. Ibarra, J. Magn. Magn. Mater. **196-197**, 649 (1999).
[27] A. del Moral and K. Kulakowski (unpublished); B. Barbara, D. Gignoux, and C. Vettier, *Lectures on Modern Magnetism* (Springer-Verlag, Berlin, 1988), p. 134; K. Kulakowski and C. Lacroix, Phys. Status Solidi B **165**, K17 (1991), and references therein.
[28] J. Inoue and M. Shimizu, J. Phys. F: Met. Phys. **15**, 1511 (1985).
[29] R. Coehoorn, Phys. Rev. B **39**, 13 072 (1989).
[30] Zong-Quan Gu and W. Y. Ching, Phys. Rev. B **36**, 8530 (1987).
[31] V. Heine, Phys. Rev. **153**, 673 (1967); J. F. Janak and A. R. Williams, Phys. Rev. B **14**, 4199 (1976).